# THE OPTIMIZATION CONDITIONS TO USE PHOTOVOLTAIC ARRAYS IN DRIVING VAPOUR COMPRESSION COOLING SYSTEM.

M.G Osman*
College of Engineering, El-Mansoura University, El-Mansoura Egypt.

ABSTRACT:

A photovoltaic powered vapour-compression air conditioner system coupled directly to 2 KW PV array was designed end tested as part of solar houses cooling program in KISR, KUWAIT. Analysis of such systems is reviewed and discussed to optimize the power matching of the mechanical load to the PV array electrical characteristics. The concept is employing a variable speed seperately excited D.C. motor. Motor starting and operation at low levels of solar insolation is enhanced by introducing switching network and variation of flux and armature resistance. Various modules are switched in parallel under high current demand conditions and at early and late hours of the day to increase the utilizability of the system. Analysis of other types of A.C and D.C motors and compressors w.r.t their corresponding starting systems are reviewed and discussed. Energy storage is incorporated in the form of chilled water (end use energy form) in order to avoid the electrical storage batteries with their high cost and low charge/discharge (round trip) efficiency.

The tests carried confirm that high array utilization can be achieved by this approach without either secondary battery storage at the array output or expensive DC-AC inverter.

## INTRODUCTION:

For solar energy to be used for air conditioning, it must be converted into mechanical power or electricity. This can be achieved by either one of two diffrent routes; Solar thermodynamic and solar photovoltaic conversion. Fig.(1). Solar photovoltaic power systems for air conditioning of buildings have recieved little attention due to the historically high cost of photovoltaic modules relative to solar thermal collectors. The projected continuing decrease in photovoltaic module costs may alter current perceptions of the role of photovoltaics in space conditioning systems.

Their are two reasons behind the present interest in solar cooling especially in hot countries like (Kuwait).

---

* On Sabbatical Leave To Solar Energy Department

They are: a- the coincidence of solar radiation and the cooling requirements of buildings affects favourably solar cooling system economics due to low storage requirements. b- effective solar cooling systems could obviate the need for electric utility capacity expansion necessary to meet the rapid growth of summer peak demands. (1)

Photovoltaic- powered air conditioning systems are generally assumed to provide D.C. electric power to a D.C -to-A.C. inverter which in turn serves all the electric demand of the building including the air conditioner. This system suffers from high cost of batteries, their low charge and discharge efficiency in addition to the expensive high capacity inverter to afford starting currents (5-8 times rated current) and low efficiency at part loads. (2)

An alternative concept is introduced in this paper which involves the direct coupling of a photovoltaic array and an air conditioner with an impedance matching maximum power point tracker (MPPT). Such a device varies the array voltage to maximize the power input into the air conditioner, compressor and consequently maintains the photovoltaic array at its maximum power point Fig.(2).

The direct coupled system relies mainly on the coincidence of insolation and the air conditioning load. Because peak cooling loads occur several hours after solar noon, diurnal buffering with chilled water storage is then desired. Similar chilled water storage concepts which chill water at night using off-peak rate electricity have been tested world wide. An advantage of this end use energy storage form is no more need to electrical batteries which in field causes the most problems. (3)

## P.V. Systems and Motor Starting Techniques:

A- If an induction motor is started at full voltage, it normally draws seven to nine times its full rated KVA during the time necessary to accelerate from stall to full speed. This starting transient determines the size of the major system components in particular the inverter. Besides if there is no storage to provide system stifness, the starting transient becomes a cruical consideration. An attractive solution is to utilize a variable voltage/ frequency motor starting scheme where the motor is started at low frequency and a correspondingly scaled voltage. The voltage and frequency are both slowly increased to the nominal running values. This procedure allows starting the motor with stall torques comparable to those from across-the-line starting but virtually with no input power transient. However this scheme of inverter plus AC motor

did not appear to be an attractive solution due to the complex electronic control system and low efficiency due to operation of motor and inverter below their design power and efficiency. Fig. 3(a,b). (4)

B- Another technique was used to start the motor at no or reduced loads and to extend the power match to lower levels of irradiance but this time this is achieved in compressor side (only piston type) not the motor side. The technique is to unload one or more cylinders during starting or even hot gas by-pass is brought into circuit and short circuiting all cylinders (Fig. 4). Should the array output fall below certain threshold limit propotional to certain threshold radiation level the motor speed shall fall and the compressor will be unloaded. As sufficient power is daveloped due to increase in insolation level then, the cylinders will be reloaded again in sequence. This technique in either loading or unloading needs again complex electronic control item and the system suffers from stability problems due to unbalance of operation at less than the designed full number of cylinders. (5)

C- Switching Networks, are used in many photovoltaic applications when start up currents are much higher than steady state currents. Also, as the solar radiation level changes throughout the day, the individual solar cell output voltages and currents will also change. In order to insure a consistent supply to the load, and to allow for differences in load conditions during start-up and steady state operating conditions; switching networks are incorporated in the solar cell array circuit.(6)

They allow various modules to be switched in parallel under high current demand conditions (motor starting) and during periods when the level of solar insolation is decreasing. Fig. (5).

## P.V. System Configuration:

The direct coupled photovoltaic air conditioning system configuration is illustrated in Fig.(6). Solar radiation I, strikes a photovoltaic array of active cell area $A_c$ and produces electric power $P_e$ at the array's maximum power point. Most of this power is consumed in a compressor and in fans to run a vapor compression system which extracts heat $Q_e$, from a cooled space with an evaporator and rejects the total thermal and electrical energy through a condencer. A simplified analysis of this system models the photovoltaic array at its maximum power point with

$$P_e = I A_c \eta_c \qquad \ldots\ldots(1)$$

$$\eta_c = \eta_c^o - \eta_c^1 (T_a + \gamma I) \qquad \ldots\ldots(2)$$

No losses are assumed for the maximum power tracker in the analysis. Both the D.C. motor and the compressor are considered as devices with fixed efficiency.(7)

The vaporcompression loop performance (carnot cycle) is given by

$$Q_e = P_e \quad CO \; P_c \qquad .....(3)$$

$$COP_c = \frac{T_s - Q_e R_e + 273}{T_a + Q_c R_c - T_s + Q_e R_e} \qquad .....(4)$$

$$Q_c = Q_e + P_e \qquad .....(5)$$

These equations may be solved to yield the evaporator heat transfer $Q_e$, as a function of the insolation and ambient temperature. A solar coefficient of performance defined as the evaporator heat transfer divided by the rate at which radiation strikes active photovoltaic cell area

$$COP_s = Q_e/I \; A_e \qquad .....(6)$$

A typical example of this performance measure is shown in Fig.(7) for a case where chilled water is stored at 5°C.

P.V. System Hardware and Performance:

The solar house at KISR was chosen to house the P.V. solar cooling components and provide the cooling load to small room (20 $m^3$). The system consisted of 2 K.W,P.V. Arrays. Out of these arrays 14 series connected solar power corporation modules were used. At standard operating conditions these modules maximum power point is 16.6 volts at 1.89 amps. Assuming no cell string mismatch or other degradation the array then produces 440 watts. The cell temperature rise above ambient is approximately 0.025 °C for each unit of insolation in watts/$m^2$.

With insolation level of 800 $Wm^{-2}$ and 32.2°C ambinet temp/the photovoltaic array cell temperature in the experimental system will equal 52.2°C. and the maximum power point output will be approximately 330 watts.

From Figure (8), the cooling capacity is determined to be 713 watts (thermal). This results in a cooling coefficient of performance of 2.25. The solar coefficient of performance is approximately 0.2, based on 800 watt per square meter insolation and 4.54 square meters of photovoltaic cells.

Parametric Analysis:

Experimental testing were applied to study the effects of:

1- Variation of flux and armature resistance,
2- Array size and inter connections on the maximum power line.

For this experiments, another type siliconcell P.V array of 300 $W_p$ power output and low voltage, high current motor was used (22 V, 15 A). The array was constructed from 36 paralled strings of 36 series connected cells in a string. I-V and P-V curves corresponding to three radiation levels are presented in Fig.(9). The maximum power lines and two lines of 90 percent of its value are drawn in the figure by dashed lines. These two lines form a quite wide area (dashed) in which the operating voltage may vary. Up ±10 per cent and more than 90 per cent of the maximum power will be delivered.

1- Variation of flux and armature resistance:

As seperately excited motor is used to give better torque-speed characteristics. The external control of the field could be implemented either:

a) an open loop method where the field current is function of shaft speed (inverse relationship).

b) closed loop feed back with a constant armature voltage as the airing point.

The transformed mechanical load in the electrical plane is thus shifted towards the maximum power line. Higher values of $\emptyset$ and $R_a$ improve the load curve at lower radiation levels and vice versa. At any rate, motor matching to a given load and a photovoltaic converter involves the choosing of proper values of $\emptyset$ and $R_a$(Fig.10).

2- Variation of array interconnections:

As the photovoltaic converter is composed of P = 36 strings connected in parallel and S = 36 cells connected in series in each string. S and P determines the voltage and current respectively. By changing the array connections we affect the locus of the maximum power line. The decrease in S (for P = const) causes $V_p$ (at maximum power) to decrease (for the same current $I_p$) and hence the maximum power line will move toward the current axis. The decrease in P (for S = const) will cause the maximum power line to move toward the voltage axis. Now since the transformed mechanical load in the electrical plane is independent of the converter, it is possible to bring the maximum power line to the vicinity of the mechanical load by choosing optimal P and S Fig.(11) shows the I-V characteristics (for the same radiation of 70 $mw/cm^2$) for

diffrent SxP matrices, their corresponding maximum power lines and the transformed load (ventilator). As an example changing P from 36 to 28 affects the system operation, the system starts to operate later in the morning (8:00 instead of 5:30) and operates shorter time during the day (11 hrs instead of 13 hrs). Besides the variation of P and S in the solar array affects the mechanical characteristics of the motor and hence the operating point. For this operately excited motor $T = C_1 I$ and $N = (u - IR)/C_2$ and thus the array current and voltage determine the motor torque and speed respectively.

CONCLUSIONS:

(1) The vapour compression cycle for airconditioning, powered by photovoltaic electricity is feasible, and is an interesting alternative for solar cooling, provided the electrical energy is not stored in an electrical battery but in an ice-bank or similar post energy use device.

(2) Starting of A.C. induction motors on photovoltaic power systems without storage battery can be achieved by using variable frequency/voltage starting scheme. Although inverters and motors can operate at high efficiencies (up to 90%); when ever they operate below their design point (maximum power) their efficiency decreases as it happens also when operating at other than their design frequency.

(3) Starting of D.C. (seperately excited) motors can be greatly enhanced by the switching networks which increase the number of parallel strings during motor starting and periods of low insolation values.

(4) Operation of the photovoltaic system close to maximum power line is very essential due to the high cost of solar cells and can be successfuly achieved by varying the motor flux or armature resistance in proportion to solar insolation level to track the maximum power line of the array.

(5) P.V. System time of utilization will be also increased by controlling the motors parameters ($\phi$, $R_a$) and proper interconnections of the solar panels.

(6) Out of the three D.C. motor types (seperate , series and shunt excited motors), the series and seperately excited motors are more compatible to the photovoltaic systems, as they have relatively high starting torque, stability and better utilization of the solar cell array as can be seen by grapho-analytical method of analysing the system in both electrical (V, I) and mechanical (N,T) planes, giving an insight of the operation and allowing

conclusions concerning the selection of system components to be formulated.

(7) System analysis in the mechanical plane reveals important information about the torque, speed, stability and optimal mechanical load. The analysis in electrical plane contributes important details about the operating voltage, power and efficiency.

REFERENCES:

1. Kern, E.C., and Millner, A.R., "Performance of a photovoltaically powered Air-Conditioning System", 14th PV conference, San Diego, CA, Coo-4094-73.

2. Mattarolo, L., "Solar Powered Air-Conditioning Systems". International Journal of Refrigeration, Volume, 5, Number 6, pp. 371-379.

3. Sheldon, B.D., "Solar Photovoltaic/Thermal (Hybrid) Energy Project", MIT, Lincoln Laboratory, Coo-4577-11.

4. Darkazalli, G. and Lawley, T.J., "Analytical and Experimental Evaluation of Solar Absorption and Vapour Compression Residential Cooling Systems, Alternative Energy Sources, Solar Energy" pp. 775-783.

5. Bilgen, E. "Solar Cooling, Proc Application of Solar Energy," Ed. D.J. Catania, 65-84, 1974.

6. Lazzaim, M.B., Baldin,, Experimental investigation of Control Modes for an Absorption chiller of low capacity. pp. 710-714.

7. Ward, D.S., Weiss, T.A., Lof, G.O. Performance of CSU Solar House Heating and Cooling System, Solar Energy, 18, 541, 1976.

NOMENCLATURE:

| | |
|---|---|
| $A_c$ | Active photovoltaic cell area ($m^2$) |
| $COP_c$ | Cooling coefficient of performance (-) |
| $COP_s$ | Solar cooling coefficient of performance (-) |
| $I$ | Insolation on collectors ($W\ m^{-2}$) |
| $P_e$ | Array electric power (W). |
| $Q_c$ | Condencer heat transfer rate (W). |
| $Q_e$ | Evaporator heat transfer rate (W). |
| $R_c$ | Condencer terminal resistance ($°C\ W^{-1}$) |
| $R_e$ | Evaporator thermal resistance ($°C.W^{-1}$) |
| $T_a$ | Ambient air temperature (°C). |
| $T_s$ | Indoor temperature (°C). |
| $\eta$ | Cell efficiency (-). |
| $\eta_c^o$ | cell efficiency at 0°C. (-) |
| $\eta_c^1$ | Cell temperature sensitivity ($°C^{-1}$) |
| $\eta_s$ | Solar heating coefficient of performance (-) |
| $\gamma$ | Cell temperature rise per unit insolation ($°C.m^2.W^{-1}$). |

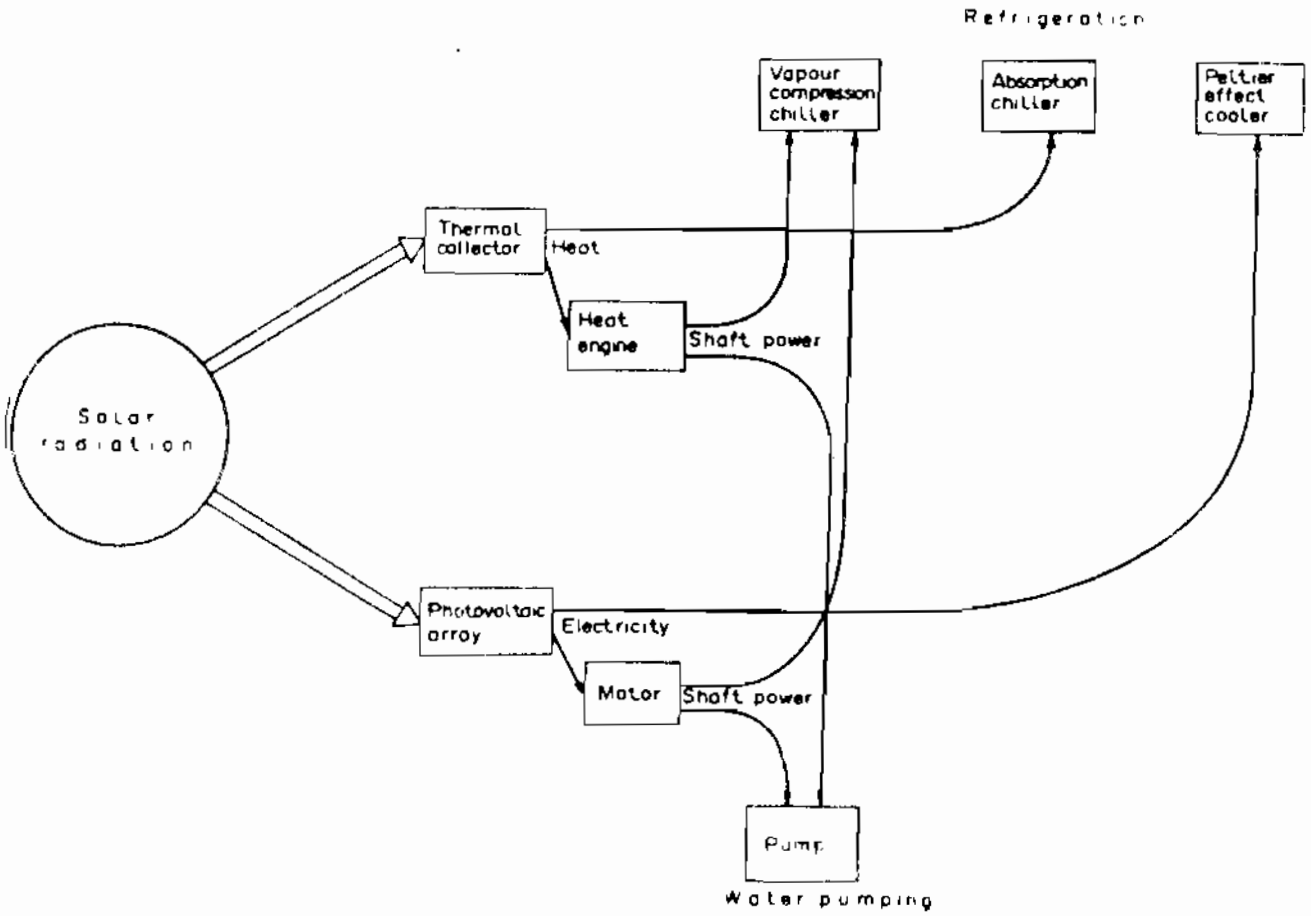


Fig.(1): Conversion routes for refrigeration and water pumping by solar energy.

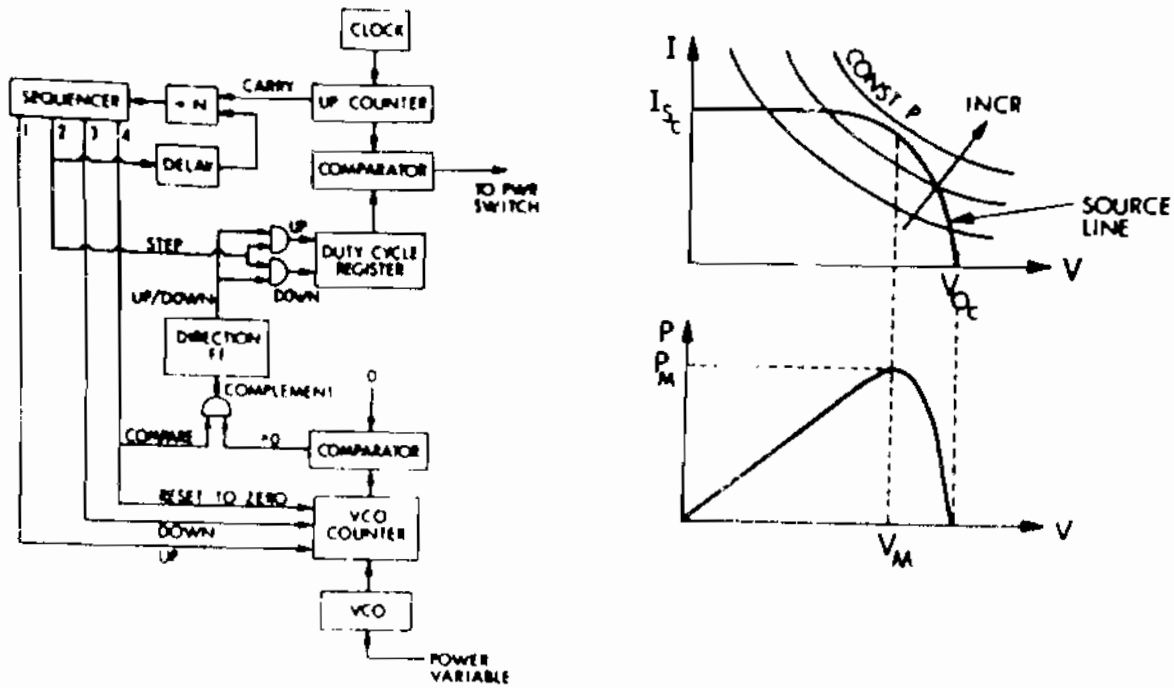


Fig.(2): Maximum power tracking algorithm.

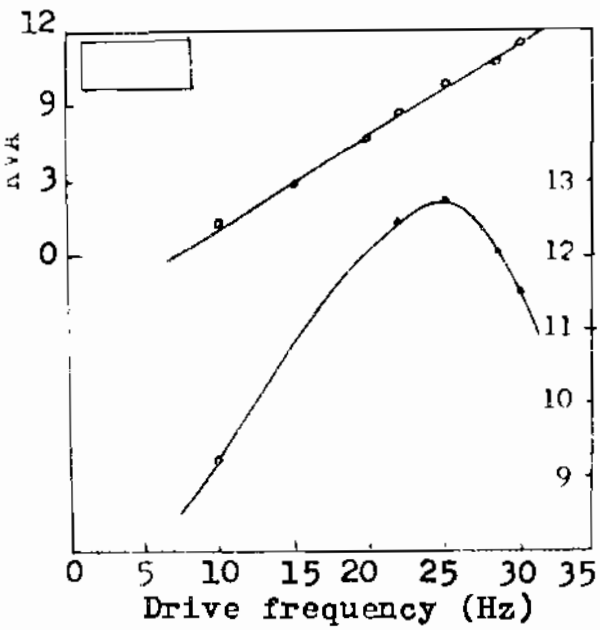


Fig.(3.a): Motor Stall Charactristic.

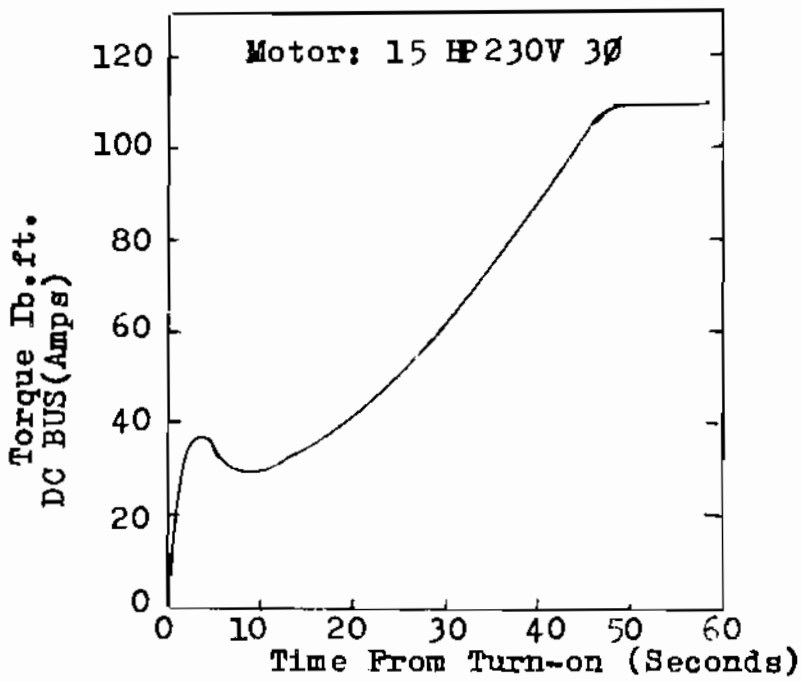


Fig.(3.b): Motor Starting Transient.

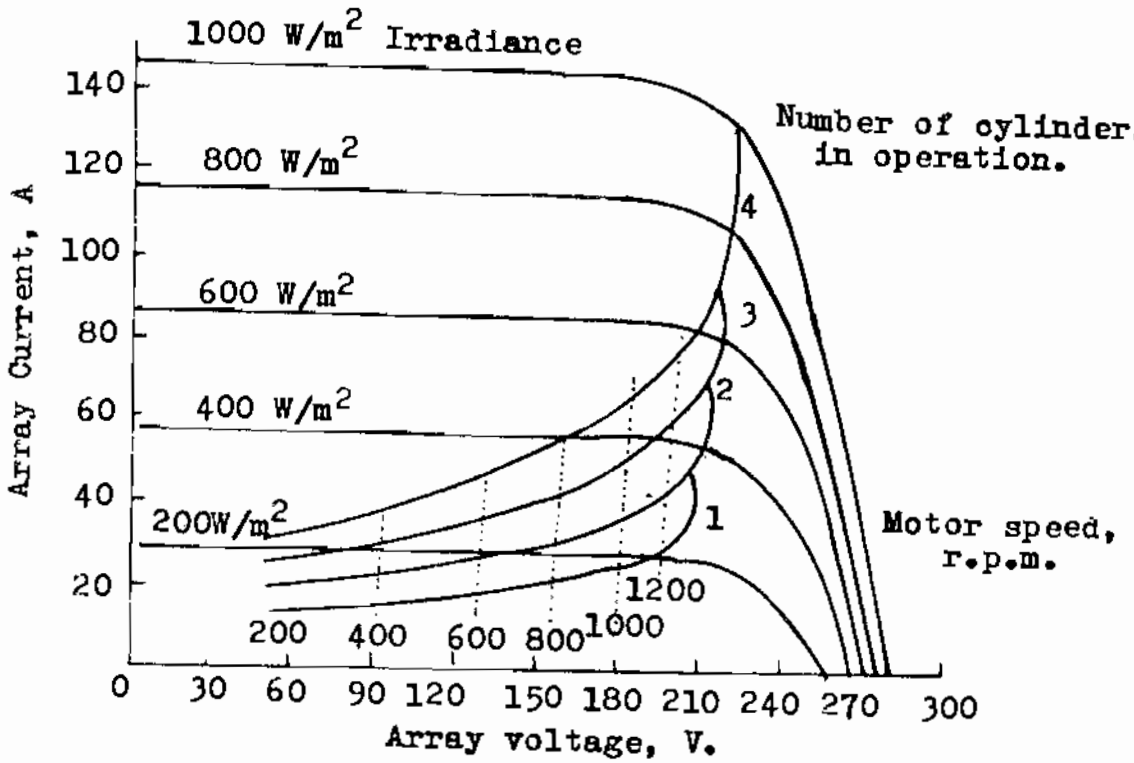


Fig. 4: Characteristics of matched system.

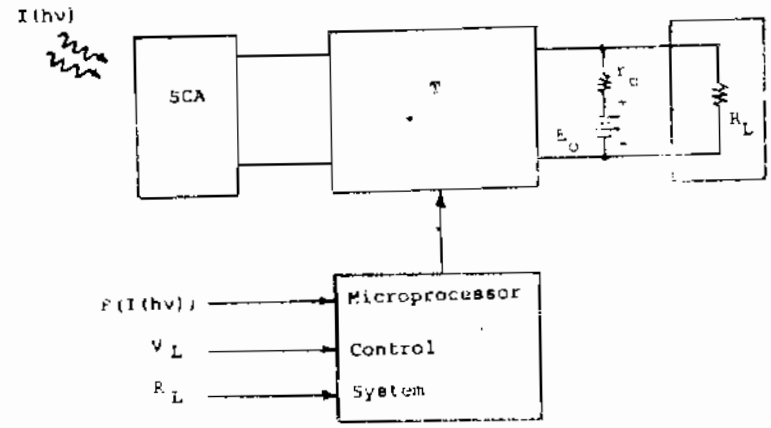


Fig.(5): Microprocessor control for Array Transformation Network to adjust for varying load conditions and varying output conditions from the SCA.

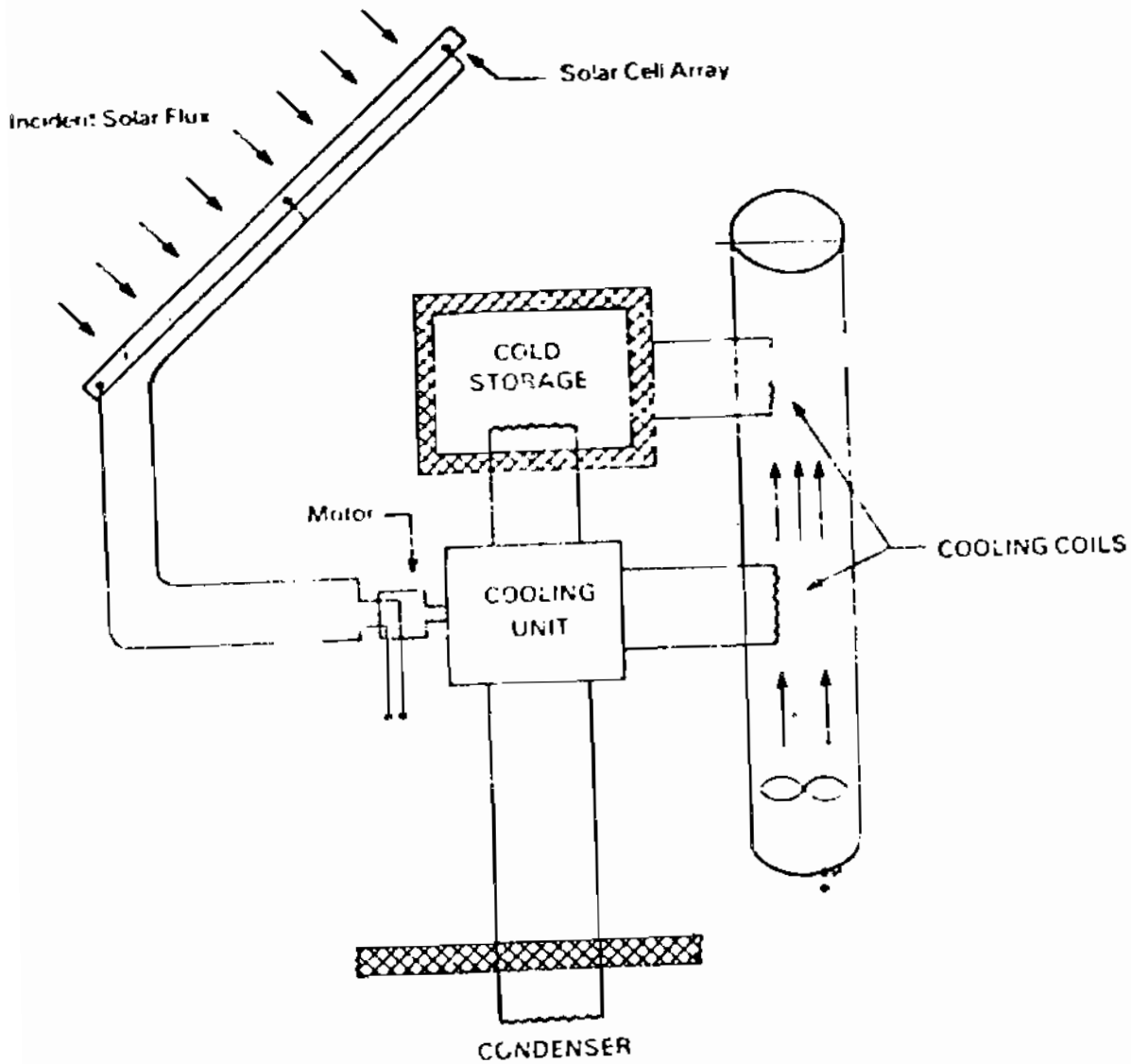


Fig.(6): Direct coupled cooling system.

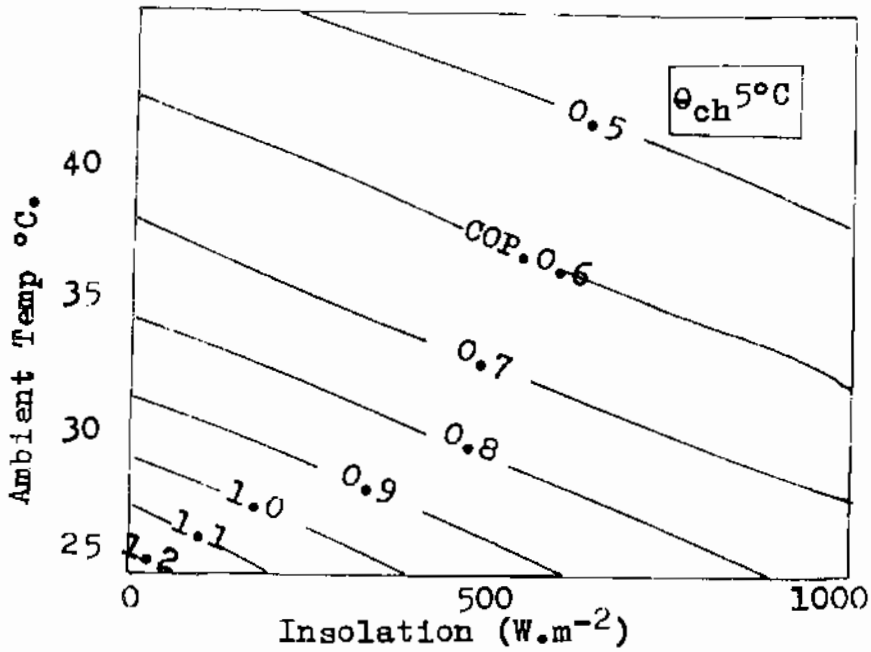


Fig.7: Solar cooling coefficient of performance as a function of temperature and insolation with 5°C chilled water.

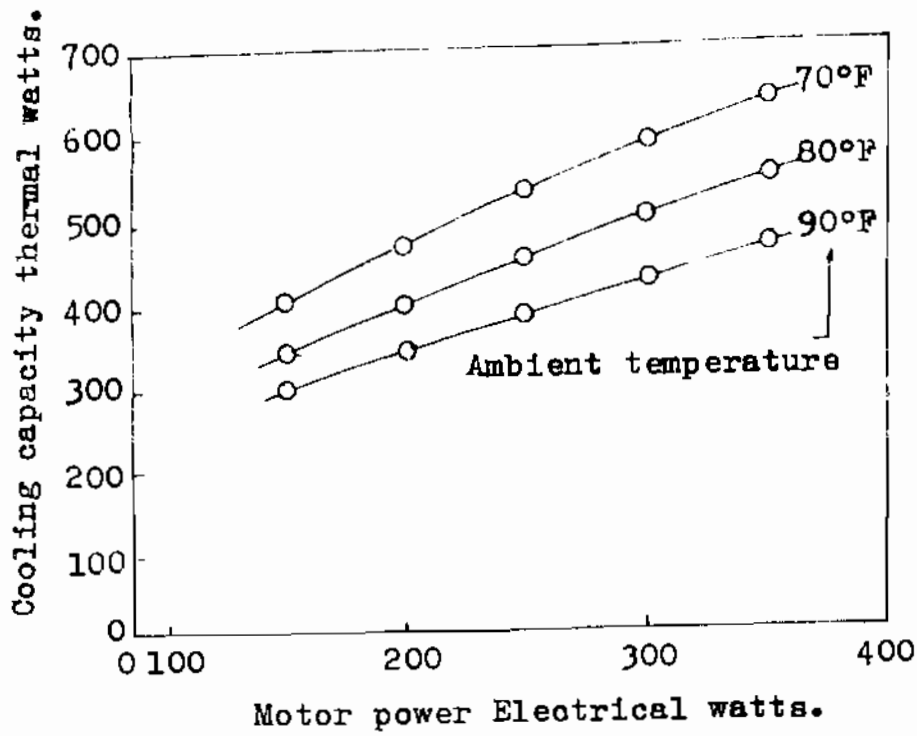


Fig. 8: Measured cooling capacity as a function of compressor electric power.

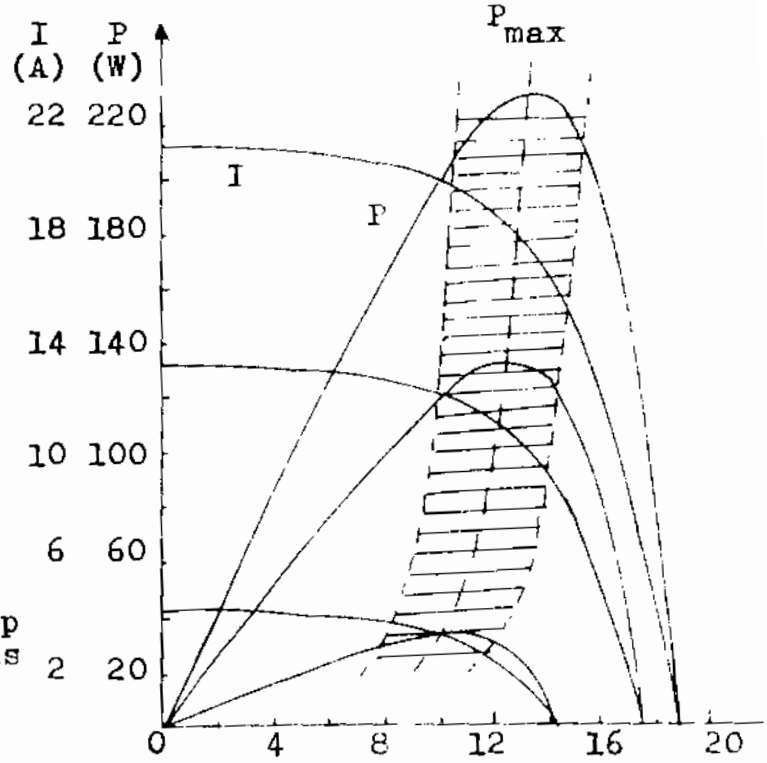


Fig. 9: I-V and P-V photovoltaic characteristics.

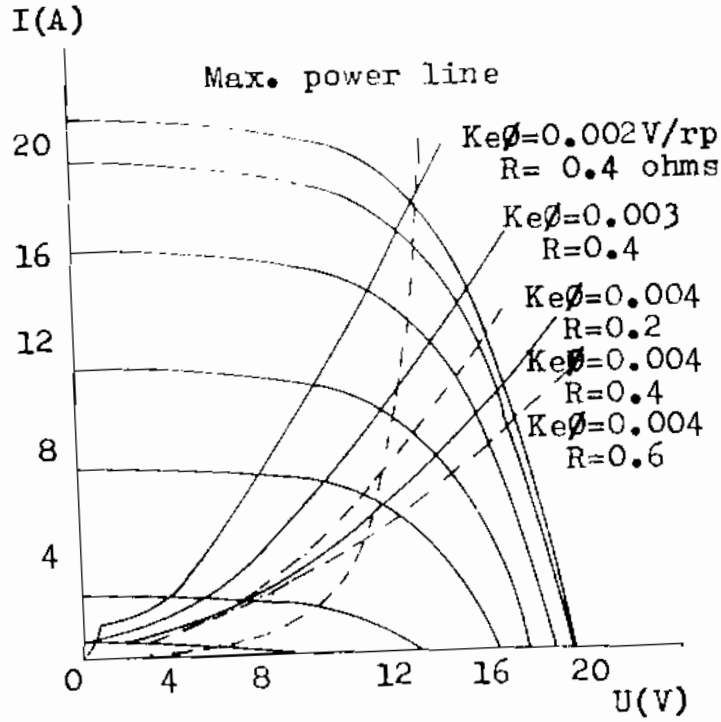


Fig.(10): Effect of the variation of R and Ø on the transformed load.

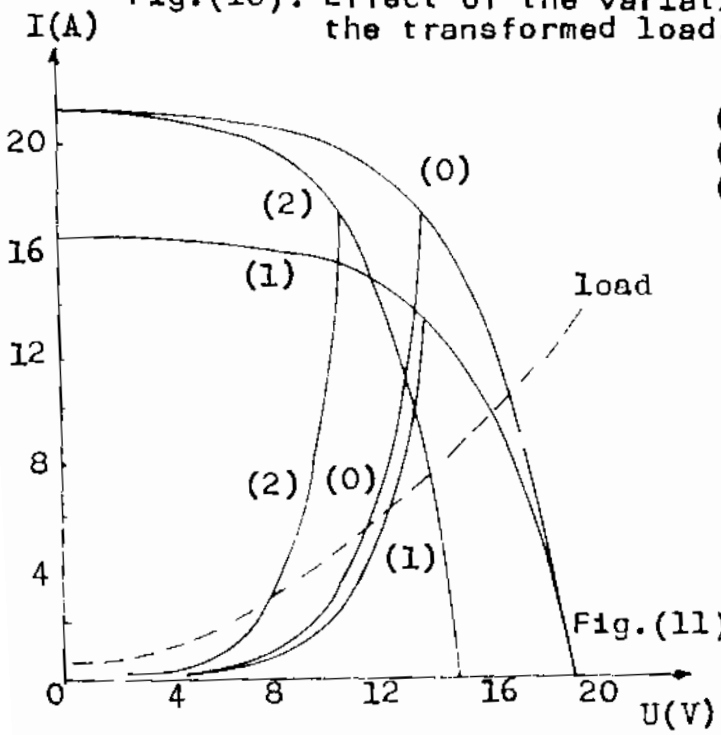


(0)-S.P = 36.36
(1) = 36.28
(2) = 28.36

Fig.(11): Effect of the array size and interconnections on the maximum power line.